Biosensors and Bioelectronics 113 (2018) 1–8

Contents lists available at ScienceDirect

Biosensors and Bioelectronics

journal homepage: www.elsevier.com/locate/bios

A cascade autocatalytic strand displacement amplification and hybridization chain reaction event for label-free and ultrasensitive electrochemical nucleic acid biosensing

Zhiqiang Chen, Ying Liu, Chen Xin, Jikuan Zhao, Shufeng Liu*

Key Laboratory of Sensor Analysis of Tumor Marker, Ministry of Education, College of Chemistry and Molecular Engineering, Qingdao University of Science and Technology, No. 53, Rd. Zhengzhou, Qingdao, Shandong 266042, China

ARTICLE INFO

Keywords:
Nucleic acid biosensor
Electrochemical detection
Strand displacement amplification
Hybridization chain reaction
Silver nanocluster

ABSTRACT

Herein, an autocatalytic strand displacement amplification (ASDA) strategy was proposed for the first time, which was further ingeniously coupled with hybridization chain reaction (HCR) event for the isothermal, label-free and multiple amplification toward nucleic acid detection. During the ASDA module, the target recognition opens the immobilized hairpin probe (IP) and initiates the annealing of the auxiliary DNA strand (AS) with the opened IP for the successive polymerization and nicking reaction in the presence of DNA polymerase and nicking endonuclease. This induces the target recycling and generation of a large amount of intermediate DNA sequences, which can be used as target analogy to execute the autocatalytic strand displacement amplification. Simultaneously, the introduced AS strand can propagate the HCR between two hairpins (H1 and H2) to form a linear DNA concatamer with cytosine (C)-rich loop region, which can facilitate the in-situ synthesis of silver nanoclusters (AgNCs) as electrochemical tags for further amplification toward target responses. With current cascade ASDA and HCR strategy, the detection of target DNA could be achieved with a low detection limit of about 0.16 fM and a good selectivity. The developed biosensor also exhibits the distinct advantages of flexibility and simplicity in probe design and biosensor fabrication, and label-free electrochemical detection, thus opens a promising avenue for the detection of nucleic acid with low abundance in bioanalysis and clinical biomedicine.

1. Introduction

The development of nucleic acid biosensor is of great importance for clinical diagnosis, food analysis, environmental monitoring, and bioterrorism (Jung and Ellington, 2014; Du and Dong, 2017; Liu et al., 2009; Smith et al., 2017). Over the past decades, different techniques such as electrochemistry, spectroscopy, surface plasmon resonance, colorimetry, and so on, have been well explored for DNA biosensor fabrication (Baaske et al., 2014; Schena et al., 1995; Zhang et al., 2017; Zhao et al., 2014; Shu et al., 2018; Qiu et al., 2017b). Among them, electrochemical method shows some prominent features including inherent signal stability, low cost, ease of calibration and miniaturization (Das et al., 2015; Drummond et al., 2003; Xiao et al., 2007; Qiu et al., 2018). Currently, the polymerase chain reaction should be the most often employed method for the amplified analysis of nucleic acid (Hindson et al., 2013; Heid et al., 1996). However it is often limited by the delicate control of temperature cycling and complex primer design. Thus the pursuit of isothermal amplification strategy for the profiling of trace amounts of nucleic acid is in high demand.

Till now, different isothermal amplification methods have been advocated for nucleic acid biosensor fabrication, which further include nuclease-based or enzyme-free strategy based on the use or not of protein enzyme (Zhao et al., 2015; Craw and Balachandran, 2012; Chen et al., 2017; Zhang et al., 2018; Qiu et al., 2017a). The nuclease-based signal amplification is usually operated by the individual or combined role of various nucleases including endonuclease, exonuclease and polymerase, etc. to contribute the signal amplification via target recycling operation (Wang et al., 2011; Guo et al., 2018; Liu et al., 2015). Especially, the autonomous replication-scission-displacement strategy by means of polymerase and nicking endonuclease could afford an isothermal exponential amplification capability toward nucleic acid detection (Weizmann et al., 2006; Chen et al., 2015; Zhang and Zhang, 2012; Yin et al., 2013; Nie et al., 2015). However, a linear DNA template is commonly used, which is not beneficial for the selective discrimination of target DNA, especially for base mismatch analysis. Also the generated DNA replicates could hybridize with the free DNA template, restricting the detection performance toward target to some extent. Furthermore, it is more prone to the fluorescence detection. Thus

* Corresponding author.
E-mail address: sliu@qust.edu.cn (S. Liu).

https://doi.org/10.1016/j.bios.2018.04.046
Received 19 February 2018; Received in revised form 3 April 2018; Accepted 18 April 2018
Available online 23 April 2018
0956-5663/

upgradation of such isothermal exponential amplification system to improve its detection sensitivity and selectivity, and adaptability with electrochemical measurement remains highly desirable. The enzyme-free amplification strategy could be regarded as another research focus for nucleic acid biosensor fabrication, which is usually designed on the basis of dynamic DNA assembly principle (Zhang and Seelig, 2011; Liu et al., 2017). The typical examples include catalytic hairpin DNA assembly (CHA) and hybridization chain reaction (HCR) strategies. The CHA is operated with the catalytic assembly of two hairpins into duplex DNA in the presence of target trigger for signal amplification (Yin et al., 2008; Li et al., 2011). However, it is often confronted with the relatively rigorous sequence design, which would easily induce a relatively high background signal owing to the potentially non-specific reaction between two hairpin substrates. The HCR is operated with the alternate assembly of two DNA hairpins in the presence of target to form a DNA concatamer. It can be used as an universal post-amplification strategy for the fabrication of various biosensors toward the analysis of nucleic acid, protein and small molecules (Ikbal et al., 2015; Dirks and Pierce, 2004; Ge et al., 2018; Zhou et al., 2018). Although these substantial advances have been made for the fabrication of amplified nucleic acid biosensors, the development of simple, isothermal and autonomous amplification system with further upgraded detection performance is still highly demanded to satisfy the requirement for the profiling of trace amounts of biomarkers.

Herein, an autocatalytic strand displacement amplification (ASDA) was firstly proposed via the combined role of nicking endonuclease (Nt.BbvCI) and Bst DNA polymerase, which was then ingeniously grafted with hybridization chain reaction (HCR)-based post-amplification strategy for the fabrication of an isothermal, ultrasensitive and label-free electrochemical nucleic acid biosensor. The developed sensing strategy includes two tandem and autonomous modules: ASDA and HCR. During the ASDA module, the target recognition with the immobilized hairpin probe (IP) on the electrode initiates the annealing of the auxiliary DNA strand (AS) with the opened IP. Then the polymerization and nicking reaction proceeds for the target recycling and generation of a large amount of intermediate DNA sequences, which could be used as target analogy to contribute the autocatalytic amplification toward target recognition events. Simultaneously, the introduced AS strand can propagate the HCR between two hairpins (H1 and H2) to form a linear DNA concatamer with cytosine (C)-rich loop region, which can facilitate the in-situ synthesis of silver nanoclusters (AgNCs) as electrochemical tags for further amplified detection. The AgNCs synthesized by C-rich loop DNA template have been reported for the fluorescent and electrochemical detection of various biomolecules (Enkin et al., 2014; Liu et al., 2013; Dong et al., 2012; Zhang et al., 2013; Yang et al., 2015; Orbach et al., 2013). With current cascade ASDA and HCR amplification strategy, the amount of in-situ synthesized AgNCs is dramatically enhanced, inducing substantially amplified current response for label-free and ultrasensitive detection of nucleic acid down to 0.16 fM.

2. Experimental section

2.1. Chemicals and materials

The nicking enzyme Nt.BbvCI (It can recognize the specific nucleotide sequence of 5′-CC↓TCAGC-3′ in a dsDNA and cut the nucleotide sequence in the arrow), Bst DNA polymerase (Large Fragment) and 10 × NEB buffer (50 mM NaCl, 10 mM Tris-HCl, 10 mM $MgCl_2$, 1 mM dithiothreitol, pH 7.9) were purchased from New England Biolabs Inc. (Ipswich, MA, USA). The deoxyribonucleoside 5′-triphosphate (dNTPs) mixture, tris(2-carboxyethyl) phosphine hydrochloride (TCEP) and fetal calf serum were obtained from Sangon Biotech Co., Ltd. (Shanghai, China). 6-Mercapto-1-hexanol (MCH) was purchased from Sigma-Aldrich (St. Louis, MO, USA). Silver nitrate ($AgNO_3$) was purchased from Aladdin Reagents Inc. (Shanghai, China). Acrylamide/bisacrylamide 39:1 40% gel stock solution, N,N,N′,N′-tetramethylethylenediamine (TEMED), and ammonium persulfate (APS) were purchased from Yantai Science and Biotechnology Co., Ltd. (Yantai, China). T safeTM dye was purchased from Shanghai Tianneng Science and Technology Co., Ltd. (Shanghai, China). The HPLC-purified DNA sequences were synthesized by Sangon Biotech. Co., Ltd. (Shanghai, China) and listed below. The immobilized hairpin probe (IP): 5′-SH-$(CH_2)_6$-TTTCCACTCTCGCAGAGACCGGCGCACAGAGGCTG AGGCGAGAGTGGTTT-3′; Target DNA (TD): 5′-TTCCTCTGTGCGCCGG TCTCTCCT-3′; One-base mismatched DNA (1MT): 5′-TTCCTCTGTGCG CCAGTCTCTCCT-3′; Three-base mismatched DNA (3MT): 5′-TTCCTCT GTGCGAGAGTCTCTCCT-3′; Non-complementary DNA (NC): 5′-CAAG AAATTTTTTCTCCGGGTCAC-3′; Auxiliary DNA strand (AS): 5′-TCAGC TGATCAGCCCACTCTCGC-3′; Target DNA2 (TD2) (It was designed to directly hybridize with IP and trigger the hybridization chain reaction event): 5′-TCA GCT GAT CAG CCC ACT CTC GCC TCA GCCTCTGTGC GCCGGTCTCT-3′; Hairpin DNA1 (H1): 5′- GCTGATCAGCCCCCCCCCC CCCTGATCTGCATCTAGAT-3′; Hairpin DNA2 (H2): 5′-TCAGCTGATCA GCATCTCCCCCCCCCCCCAGATGCAGA-3′; H1 without the C-rich region: 5′- GCTGATCAGTTAGATTAGATTCTGATCTGCATCTAGAT-3′; H2 without the C-rich region: 5′-TCAGCTGATCAGCATCTTTAGATT AGAT TAGATGCAGA-3′. All other reagents were of analytical grade without further purification. The used target DNA and mutated sequence is related with a tumor suppressor gene, P53 exon8 DNA. The P53 gene is a crucial biomarker in early cancer diagnosis and treatment, and known as “the guardian of gene” (Ko and Prives, 1996; Batchelor et al., 2008). All solutions were prepared with deionized water obtained from a Milli-Q water purification system (Millipore Corp., Bedford, MA, USA) with a resistivity of 18.2 MΩ cm.

2.2. DNA immobilization on the electrode surface

The gold electrode (2 mm diameter) was sequentially polished with 0.3 and 0.05 μm alumina slurries to obtain a mirror surface, followed by sonication in ethanol and deionized water for 5 min, respectively, to remove the residual alumina powder. Then, the electrode was electrochemically scanned in 0.5 M H_2SO_4 solution within a potential window between − 0.2 and + 1.5 V at a scan rate of 100 mV/s till a stable cyclic voltammogram was obtained. All the DNA sequences were heated to 90 °C for 5 min and then allowed to cool to room temperature for at least 2 h before use. The treated electrode was incubated in 50 μL immobilization buffer (20 mM Tris-HCl, 0.1 M NaCl, 10 mM TCEP, pH 7.4) containing 1 μM IP at room temperature for 4 h (Other concentrations of IP including 0.1, 0.5, 2.0 and 5.0 μM were also studied for the immobilization optimization). Then the resulting IP modified electrode was blocked with 1 mM MCH solution for 30 min to remove the nonspecific adsorbed DNA.

2.3. Autocatalytic strand displacement amplification and hybridization chain reaction

The IP modified electrode was incubated with 50 μL 1 × NEB buffer containing 1 μM auxiliary strand (AS), 10 U nicking endonuclease, 8 U Bst polymerase, 200 μM dNTPs and various concentrations of target DNA for 80 min at 37 °C. Followed by washing with 10 mM Tris-HCl (500 mM NaCl, 1 mM $MgCl_2$, pH 7.4), the electrode was incubated into the mixture of H1 (0.5 μM) and H2 (0.5 μM) in 10 mM Tris-HCl (500 mM NaCl, 1 mM $MgCl_2$, pH 7.4) for 2.5 h at room temperature. The sensors were then washed with Tris-HCl buffer and dried. Afterward, 10 μL of $AgNO_3$ solution (100 μM) in citrate buffer (20 mM sodium citrate, pH 7.0) was dropped on the electrode surface for 20 min in dark. Subsequently, 2 μL of fresh $NaBH_4$ solution (500 μM) in citrate buffer was added on the electrode surface at room temperature for 1 h in dark to reduce $AgNO_3$ to AgNCs.

2.4. Electrochemical measurements

All electrochemical experiments were performed with a CHI 660D electrochemical workstation (CH Instruments, Shanghai, China) at room temperature by using a three-electrode system consisting of the modified gold electrode, a platinum wire auxiliary electrode, and a Ag/AgCl reference electrode. The DPV measurements were carried out in PBS buffer (0.15 M, pH 5.5) by scanning the potential from 0.0 to 0.4 V with the pulse amplitude of 50 mV, pulse width of 25 ms and sampling width of 16.7 ms. The electrochemical impedance spectra (EIS) experiments were measured in 5 mM $Fe(CN)_6^{3-/4-}$ solution containing 1 M KCl with the frequency range from 0.1 Hz to 10 kHz.

2.5. Polyacrylamide gel electrophoresis

A 17.5% polyacrylamide gel was obtained by mixing 3.5 mL 40% gel solution (39:1), 160 μL 50 × TAE Buffer, 80 μL 10% APS, 4 μL TEMED and 4256 μL deionized water. Then, the polyacrylamide gel electrophoresis (PAGE) experiment was carried out in 1 × TAE buffer at 180 V for 3 min and 135 V for 90 min. Afterward, the gels were scanned using a FR-980A gel image analysis system (Shanghai, China).

3. Results and discussion

3.1. Design principle of the nucleic acid biosensing strategy

Herein, an autocatalytic strand displacement amplification strategy (ASDA) was proposed for the first time and effectively coupled with the successive hybridization chain reaction (HCR) to construct an ultrasensitive and label-free electrochemical nucleic acid biosensor, which was schematically illustrated in Fig. 1. The whole sensing strategy could be divided into two tandem modules of ASDA and HCR. Firstly, a thiol group-functionalized hairpin DNA (denoted as IP) was designed and immobilized onto the gold electrode surface by a Au-S interaction. The IP includes the target-binding sequence in the loop region (blue color) and the recognition domain for the nicking endonuclease Nt.BbvCI (cyan color). The target DNA could hybridize with the loop region of IP and made the IP stem open. Then the auxiliary DNA strand (AS) as an engaging primer annealed with the exposed IP stem and allowed polymerization from 3′-end of AS induced by Bst polymerase, which displaced the target DNA to participate into the next cycle of hybridization process. Simultaneously, a new duplex DNA with an integrated recognition site of Nt.BbvCI was produced according to the IP template, which can be nicked by Nt.BbvCI. The further polymerization from the nicks by Bst polymerase could proceed for an autonomous cleavage-replication-displacement reaction process, accompanied with the generation of a large amount of intermediate DNA fragments (Weizmann et al., 2006; Chen et al., 2015; Zhang and Zhang, 2012; Yin et al., 2013; Nie et al., 2015). These intermediate DNA fragments possess the partially identical base sequences with target DNA and could be used as target analogy to further propagate the hybridization recognition and amplification process. It should be noted that these intermediate DNA fragments would be not automatically produced in the absence of target DNA. Also these intermediate DNA fragments synthesized according to the template of IP should be not present in the real sample. Thus they would not interfere with the target DNA detection but could evidently amplify the detection toward target DNA. The proposed ASDA strategy can be subdivided into the target recycling module, and the cascade autocatalytic isothermal exponential amplification module. During ASDA process, the introduced AS strand is not only used as a primer, but also possesses an emerging DNA fragment at 5′-terminus, which can autonomously trigger the successive HCR reaction between two hairpins (H1 and H2) with cytosine (C)-rich loop to form a linear DNA concatamer on the electrode. The multiple C-rich loops on the DNA concatamers facilitated the formation of silver nanoclusters (AgNCs) upon incubation with $AgNO_3$ and $NaBH_4$. These in-situ synthesized AgNCs could be electrochemically oxidized for the signal readout and further amplification toward target detection.

3.2. Electrochemical characterization of fabricated DNA biosensor

The feasibility of the developed electrochemical DNA biosensor for target DNA detection was examined and shown in Fig. 2A. In the absence of target DNA, the autocatalytic strand displacement amplification would be inhibited and the subsequent hybridization chain reaction on the electrode surface could not occur for the generation of in-situ synthesized AgNCs. It could be seen that only a small background current response at about 0.22 V was observed (curve a in Fig. 2A), which could be attributed to the direct adsorption of Ag^+ on the self-assembled monolayer of IP by electrostatic interaction and reduction by $NaBH_4$. In the presence of target DNA, a distinctly amplified DPV current response was obtained (curve d in Fig. 2A), which was due to the electro-oxidation of the in-situ synthesized numerous AgNCs on the DNA concatamers after cascade ASDA and HCR process. The further

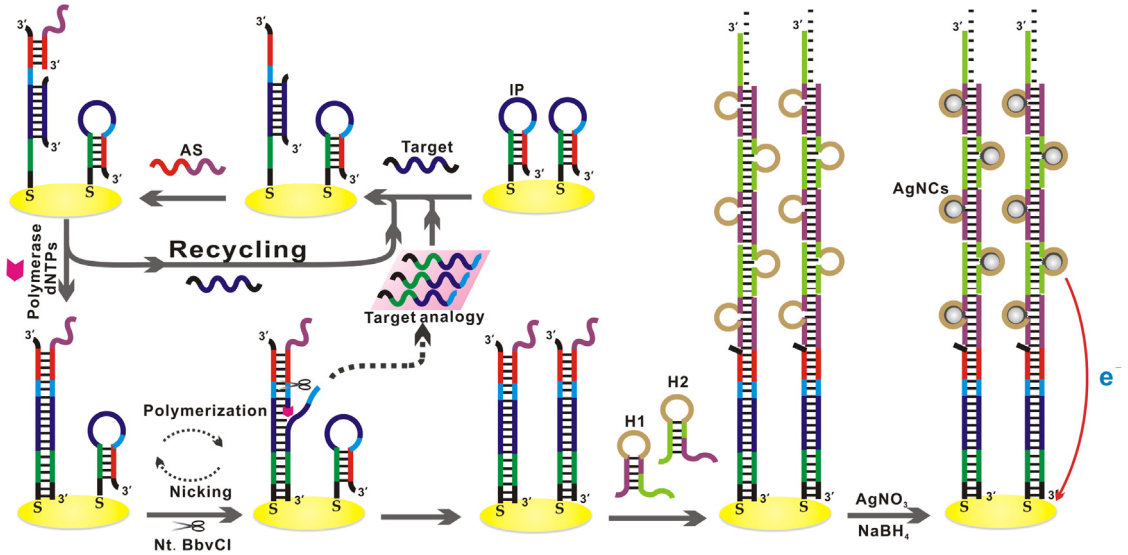

Fig. 1. Schematic illustration of the cascade ASDA and HCR strategy for nucleic acid biosensing. (For interpretation of the references to color in this figure, the reader is referred to the web version of this article.)

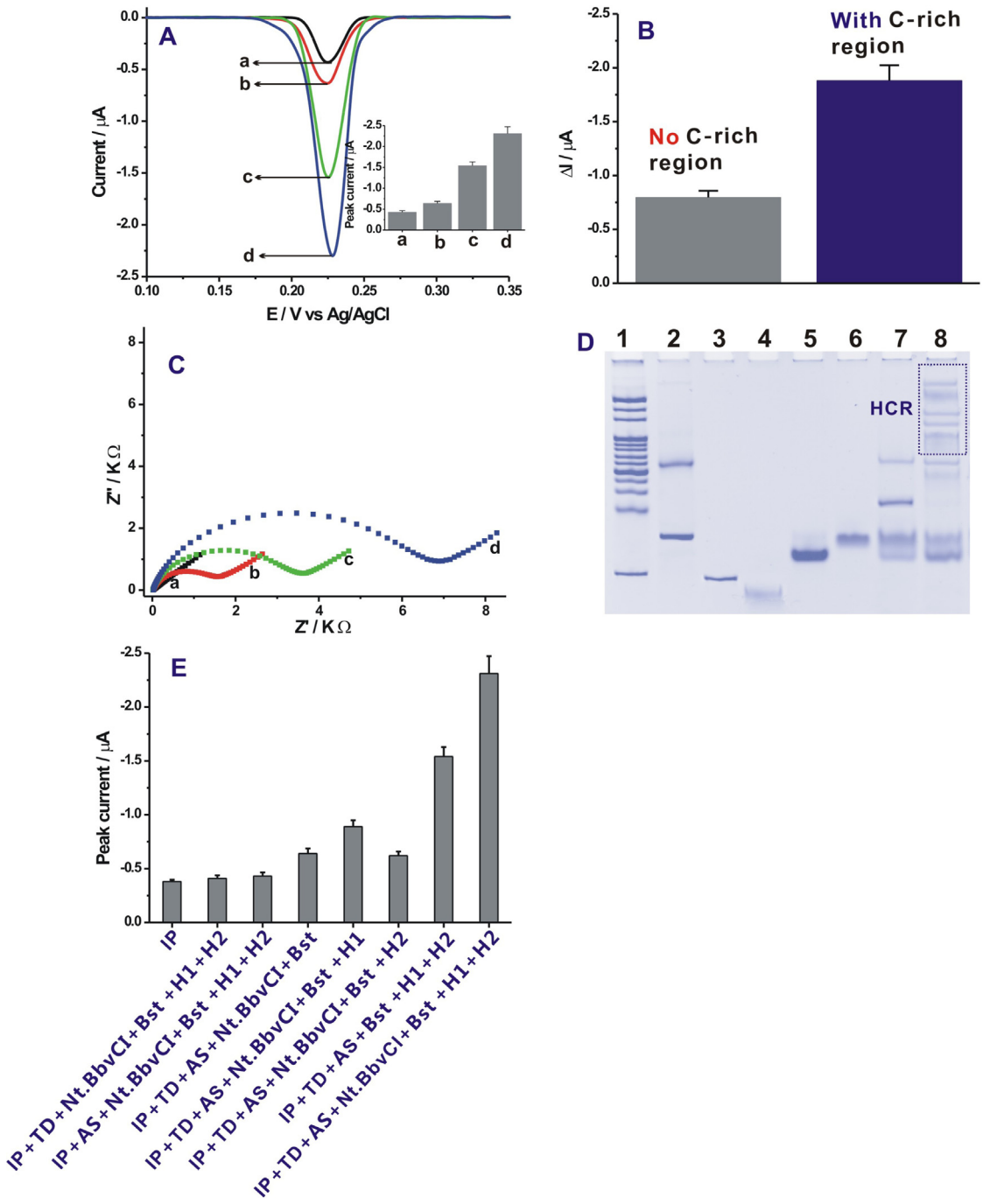

Fig. 2. (A) The DPV responses of the fabricated electrochemical nucleic acid biosensor toward blank (a) and 10 pM target DNA (d). The curves (b) and (c) are for the control experiments conducted in the absence of both H1 and H2, in the absence of nicking endonuclease (Nt.BbvCI), respectively. Inset shows the corresponding DPV peak currents. (B) Current change of the nucleic acid biosensor by using H1 and H2 with or without C-rich region ($\Delta I = I - I_0$; the I and I_0 represents the DPV peak current in the presence of or no 10 pM target DNA). The error bars were obtained based on three repetitive experiments. (C) EIS of the different modified electrodes. The curves were obtained for bare gold electrode (a), the IP and MCH modified electrode (b), the recognition toward 10 pM target DNA in the presence of nicking endonuclease and Bst polymerase (c), the further HCR between H1 and H2 (d). (D) Non-denaturing PAGE analysis: DNA marker (lane 1), IP (lane 2), target DNA (lane 3), AS strand (lane 4), H1 (lane 5), H2 (lane 6), target DNA + IP + H1 + H2 (lane 7), AS + H1 + H2 (lane 8). (E) The detailed histogram of electrochemical responses obtained under different experimental conditions. The used concentrations for target DNA (TD), assistant DNA strand (AS), Nt.BbvCI, Bst polymerase, H1 and H2 are 10 pM, 1 μM, 10 U, 8 U, 0.5 μM and 0.5 μM, respectively. Error bars show standard deviations of three repetitive measurements.

control experiment in the presence of target DNA but no H1 and H2 showed only a slightly increased current response compared with that of IP immobilized electrode (curve b in Fig. 2A). In this case, no HCR occurred for the DNA concatamer formation on the electrode, and only the duplex DNA could be obtained by ASDA process, which could adsorb more amounts of Ag^+ for the increased current response. We also conducted the target detection in the presence of only polymerase but no nicking endonuclease. The electrochemical response was evidently lower than that in the coexistence of nicking endonuclease and polymerase (curve c in Fig. 2A). The detailed control experiments conducted under different conditions were also shown in Fig. 2E. This fully evidenced the signal amplification ability of the cascade ASDA and HCR strategy for target detection. Also, we employed H1 and H2 without the C-rich loop region for HCR assembly as a comparison. The current

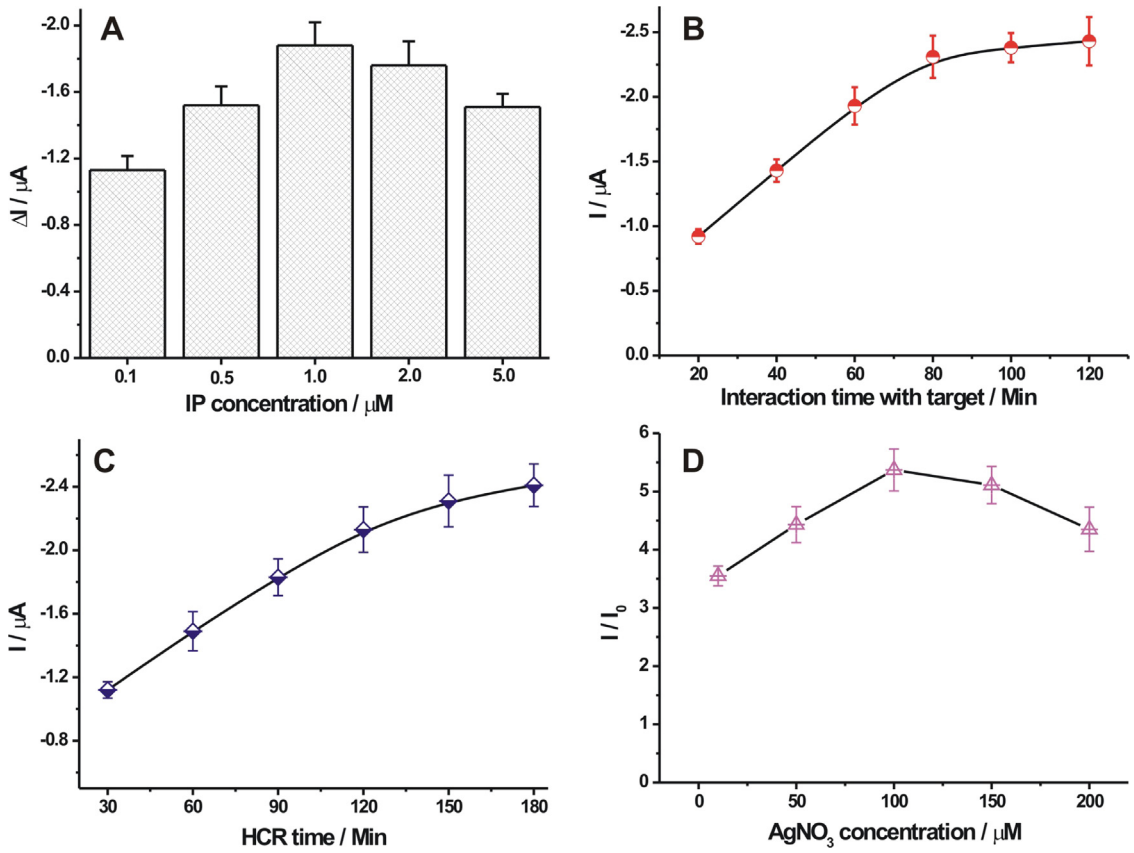

Fig. 3. (A) Optimization of IP immobilization concentration. The used IP concentrations were 0.1, 0.5, 1.0, 2.0 and 5.0 μM, respectively. (B) Time optimization for ASDA process. The studied reaction time was 20, 40, 60, 80, 100, and 120 min, respectively. (C) Time optimization for HCR process. The reaction time for HCR was 30, 60, 90, 120, 150 and 180 min, respectively. (D) The effect of $AgNO_3$ concentration on electrochemical response toward target DNA. The used $AgNO_3$ concentrations were 10, 50, 100, 150, and 200 μM, respectively. The target concentration in Fig. A–D was 10 pM Error bars show standard deviations of three repetitive measurements.

response was dramatically lower than that by using H1 and H2 with C-rich loop region (Fig. 2B). This could be explained that the formed DNA concatamer without C-rich loop region only increased the adsorption of Ag^+ instead of the formation of AgNCs.

EIS is an effective method to characterize the conductivity of the electrode surface with the use of $[Fe(CN)_6]^{3-/4-}$ in the solution as a classical redox probe. The diffusion and charge transfer ability of this redox probe toward electrode surface for impedance information could well reflect the stepwise biosensor fabrication process. The semicircle diameter in EIS diagram at higher frequencies corresponds to the charge-transfer resistance (Rct), and the linear part at lower frequencies is related to the diffusion process. The EIS characterization was shown in Fig. 2C. An almost straight line could be obtained for the bare electrode, indicating a diffusion-controlled electron transfer process on the bare gold electrode surface (curve a in Fig. 2C). After the self-assembly of IP and MCH monolayer on the electrode, the Rct was obtained as about 1562 Ω, which could be attributed to the diffusion repulsion of $[Fe(CN)_6]^{3-/4-}$ from the electrode surface by the DNA and MCH monolayer (curve b in Fig. 2C). After ASDA operation on the electrode in the presence of target DNA and AS, the Rct was increased to be about 3620 Ω (curve c in Fig. 2C). The generated DNA duplex on the electrode by ASDA process increased the negative charge and enhanced the electrostatic repellence of $[Fe(CN)_6]^{3-/4-}$ from the electrode. Also the protruding ssDNA fragment after ASDA process might offer an additional restraint for the diffusion of $[Fe(CN)_6]^{3-/4-}$ toward the electrode surface. After further HCR on the electrode surface, an evidently increased Rct value of about 6907 Ω could be observed (curve d in Fig. 2C), indicating the formation of DNA concatamers on the electrode for the distinct diffusion suppression of $[Fe(CN)_6]^{3-/4-}$ toward the electrode surface. The EIS experiments provided further beneficial supports for the nucleic acid biosensor fabrication process by the proposed cascade ASDA and HCR strategy. The HCR between H1 and H2 triggered by AS strand was also monitored by non-denaturing polyacrylamide gel electrophoresis experiment (PAGE) (Fig. 2D). A series of DNA bands with molecular weight over 500 bp could be obtained (lane 8), suggesting the AS-triggered HCR events.

3.3. Optimization of experimental conditions

To reveal the best sensing performance, the experimental conditions including the immobilization concentration of IP, ASDA reaction time, HCR time and $AgNO_3$ concentration were optimized (Fig. 3). The immobilization concentration of IP was firstly optimized based on the electrochemical response toward target DNA (Fig. 3A). An immobilization concentration of 1 μM IP could achieve the better electrochemical response than that at other immobilization concentration. A higher immobilization concentration might increase the assembly density of IP on the electrode surface. But it would be not beneficial for the cascade ASDA operation owing to the steric hindrance effect. The time dependence of the ASDA and HCR process for target response were shown in Fig. 3B and C, respectively. The optimized ASDA reaction time and HCR time was determined as 80 min and 2.5 h, respectively. The used $AgNO_3$ concentration was also optimized on the basis of the signal-to-noise ratio (Fig. 3D). A maximum I/I_0 (I and I_0 represented the DPV peak current in the presence of or no 10 pM target DNA, respectively) could be obtained at a 100 μM $AgNO_3$. This indicated that the synthesis of AgNCs could reach the saturation at the $AgNO_3$ concentration higher than 100 μM. A further increased concentration of $AgNO_3$ would cause

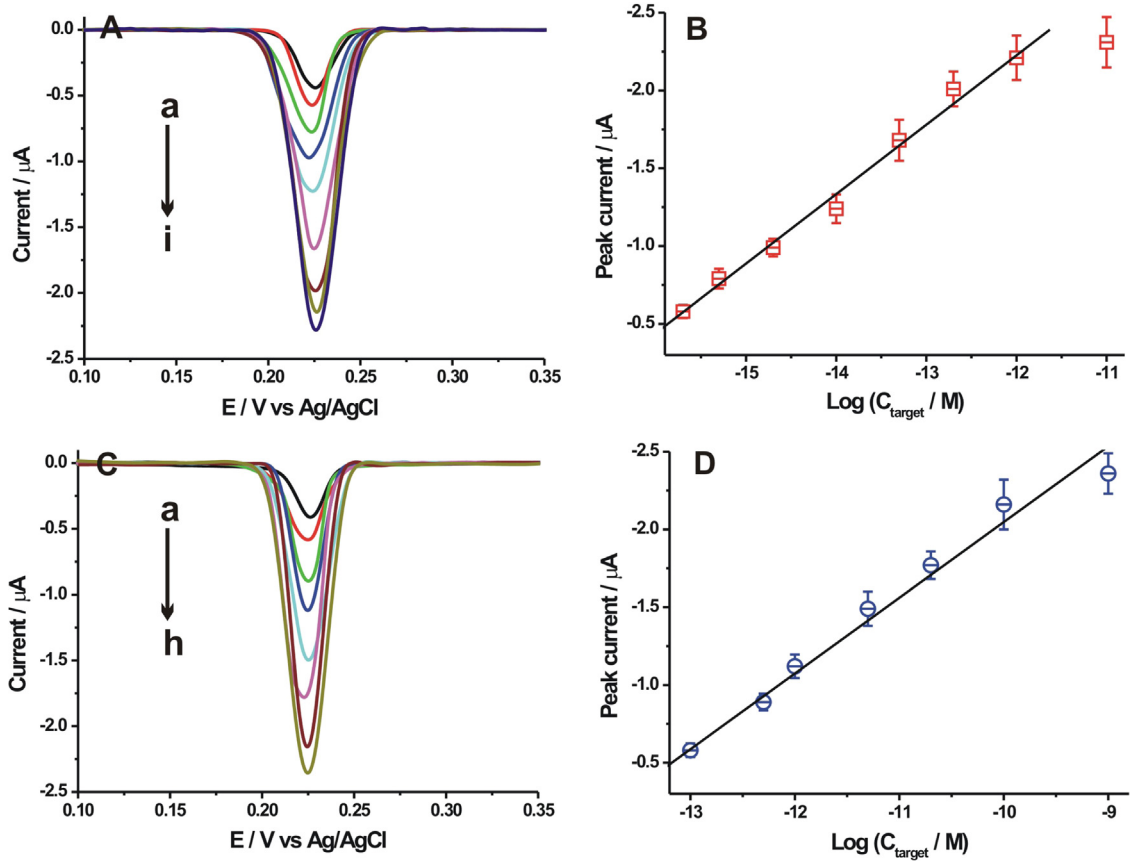

Fig. 4. (A) DPV responses toward different concentrations of target DNA by using cascade ASDA and HCR strategy. The target DNA concentration: a, 0 M; b, 0.2 fM; c, 0.5 fM; d, 2 fM; e, 10 fM; f, 50 fM; g, 0.2 pM; h, 1 pM; i, 10 pM, respectively. (B) The linear relationship between the DPV peak current and the logarithm value of target DNA concentration. (C) DPV responses toward different concentrations of target DNA by using polymerase-guided target recycling and HCR strategy. The target DNA concentration: a, 0 M; b, 0.1 pM; c, 0.5 pM; d, 1 pM; e, 5 pM; f, 20 pM; g, 0.1 nM; h, 1 nM, respectively. (D) The linear relationship between the DPV peak current and the logarithm value of target DNA concentration. Error bars represent standard deviations of three repetitive measurements.

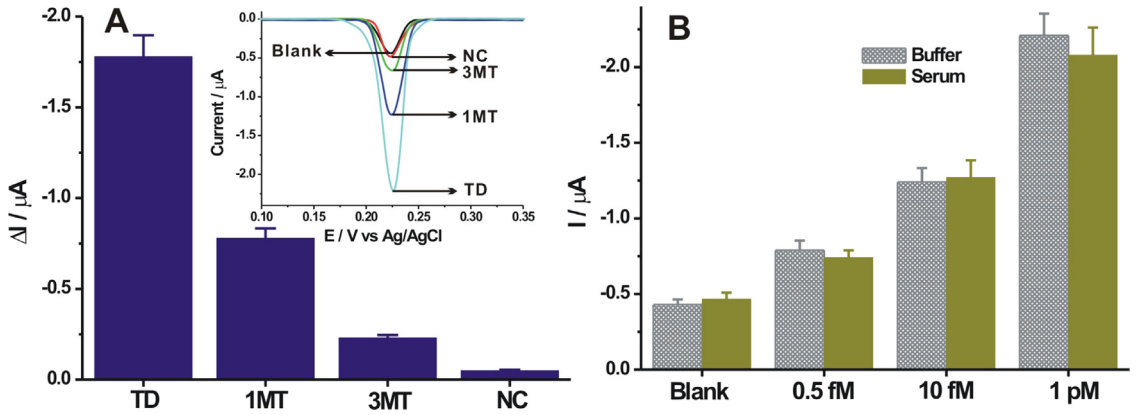

Fig. 5. (A) The current responses ($\Delta I = I - I_0$; the I and I_0 represents DPV peak current for target and blank solution, respectively) toward 1 pM complementary target DNA (TD), single-base mismatched DNA (1MT), three-base mismatched DNA (3MT) and non-complementary DNA (NC). Inset shows the corresponding DPV responses obtained at different DNAs. (B) Bar chart of DPV peak currents obtained at different concentrations of target DNA spiked in the 10% diluted fetal calf serum and buffer. Error bars represent standard deviations of three repetitive measurements.

an increased background signal, deteriorating the electrochemical response toward target.

3.4. Detection performance of the developed electrochemical DNA biosensor

To investigate the analysis capability of the fabricated electrochemical nucleic acid biosensor, the detection toward a series of different concentrations of target DNA ranged from 0 to 10 pM was conducted. As shown in Fig. 4A, the DPV peak current dynamically increased with the concentration increase of target DNA from 0.2 fM to 10 pM, indicating that the cascade ASDA and HCR process was highly dependent upon the target DNA concentration. Fig. 4B shows the calibration curve between the DPV peak current and the target DNA concentration. A linear relationship between the current intensity and the logarithm value of target DNA concentration ranged from 0.2 fM to 1 pM could be plotted according to a regression equation of Y = −7.58

to 0.45 log X (Y and X indicated the DPV peak current and target DNA concentration, respectively. The unit of X is M) with a correlation coefficient of about 0.9957. The low detection limit was defined as about 0.16 fM on the basis of 3 times the standard deviation of the background response, which was lower than most of reported nucleic acid biosensors (Table S1). Also, the relative standard deviations (RSDs) obtained toward 0.5 fM, 10 fM and 1 pM target DNA were about 7.6%, 7.2% and 6.3%, respectively, based on five repetitive measurements, suggesting a relatively good reproducibility of our proposed strategy for target DNA detection. To further prove the signal amplification effect of current cascade ASDA and HCR strategy, the target detection was also conducted in the case of no nicking endonuclease Nt.BbvCI. In this case, only polymerase-guided target recycling and successive HCR-based post-amplification contributed for target detection. The electrochemical responses at different concentrations of target DNA were shown in Fig. 4C. The current intensity also increased with the concentration increase of target DNA from 0 to 1 nM. The linear plot between the DPV peak current and the logarithm value of target DNA concentration from 0.1 pM to 1 nM could be obtained with a correlation coefficient of 0.9941 (Fig. 4D). The detection limit by this polymerase-guided target recycling and HCR was achieved as about 0.065 pM, which was evidently higher than that by the cascade ASDA and HCR strategy. Also, the HCR only amplification strategy was explored for DNA detection. Herein, a model target DNA2 (TD2) was designed, which could hybridize with and open the IP, and directly initiate the successive HCR between H1 and H2. The detection performance toward TD2 was shown in Fig. S1. A linear relationship between the DPV peak current and the logarithm value of TD2 concentration from 5 pM to 100 nM could be obtained. The detection limit toward TD2 by HCR only amplification strategy was about 2.88 pM Compared with the HCR only or polymerase-guided target recycling and HCR strategy, the proposed cascade ASDA and HCR strategy thus exhibited a prominent signal amplification ability toward target detection. The stability of the IP modified electrode for target detection had been also studied. After its storage in the refrigerator at 4 °C for 10 days, the electrochemical response could remain about 89.3% of its initial response toward 10 pM target DNA based on six independent experiments, demonstrating a relatively good stability of the IP modified electrode for target DNA detection.

3.5. Selectivity of fabricated electrochemical DNA biosensor

The selectivity of the developed electrochemical DNA biosensor was also studied by using different DNA sequences including complementary target DNA (TD), single-base mismatched target (1MT), three-base mismatched target (3MT) and non-complementary DNA (NC). As shown in Fig. 5A, the NC showed almost the same response with that of the blank solution. The current responses toward 1MT and 3MT were about 43.8% and 13% of that for complementary target DNA at the same concentration of 1 pM, respectively. These results indicated a good detection selectivity of the nucleic acid biosensor toward target DNA and the potential for base mutation analysis. To further explore its practical utility of the nucleic acid biosensor, the target DNA detection was also conducted in the 10% diluted serum (Fig. 5B). It could be seen that the electrochemical responses toward target DNA spiked in the diluted serum were basically comparable with that in the buffer, and also the current intensity increased with the concentration increase of spiked target DNA in the diluted serum. The relative standard deviations were further obtained as 9.2% and 8.7% for 10 fM and 1 pM target DNA spiked in the diluted serum, respectively, based on five repetitive measurements, demonstrating an acceptable reproducibility of the fabricated biosensor for target detection in the serum matrix. Considered with the increasing attention on the circulating nucleic acids present in the blood of patients (Das et al., 2015), the currently fabricated biosensor may hold a promising potential for the direct nucleic acid analysis in the relatively complex biological sample to serve disease diagnosis.

4. Conclusions

Herein, an isothermal, label-free and ultrasensitive electrochemical biosensor was developed by using a cascade autocatalytic strand displacement amplification (ASDA) and hybridization chain reaction (HCR) strategy. The ASDA was autonomously operated by nicking endonuclease and polymerase, accompanied with the target recycling and the generation of a large amount of analogous target sequences to execute autocatalytic strand displacement amplification. The successive HCR induced the formation of linear DNA concatamers on the electrode, which possessed a large amount of C-rich loops to facilitate the in-situ synthesis of silver nanoclusters (AgNCs) as electrochemical tags for further amplification toward target responses. The current modular and cascade operation including ASDA and successive HCR process concertedly endows the target detection with a high sensitivity and confidence. A low detection limit of about 0.16 fM with an excellent selectivity toward target DNA could be realized. The developed biosensor also demonstrates the distinct advantages of the flexibility in sequence design, simplicity in biosensor fabrication and label-free detection. It thus opens a promising avenue for the fabrication of ultrasensitive electrochemical DNA biosensor and holds a huge potential in bioanalysis and clinical diagnostics.

Acknowledgements

This work was funded by the National Natural Science Foundation of China (No. 21475072), the Natural Science Foundation of Shandong Province of China (Nos. JQ201704 and ZR2015JL007), and the Key Research and Development Program of Shandong Province of China (2016GSF201208).

Appendix A. Supporting information

Supplementary data associated with this article can be found in the online version at http://dx.doi.org/10.1016/j.bios.2018.04.046.

References

Baaske, M.D., Foreman, M.R., Vollme, F., 2014. Nat. Nanotechnol. 9, 933–939.
Batchelor, E., Mock, C.S., Bhan, I., Loewer, A., Lahav, G., 2008. Mol. Cell 30, 277–289.
Chen, A., Gui, G.F., Zhuo, Y., Chai, Y.Q., Xiang, Y., Yuan, R., 2015. Anal. Chem. 87, 6328–6334.
Chen, J., Tang, L., Chu, X., Jiang, J., 2017. Analyst 142, 3048–3061.
Craw, P., Balachandran, W., 2012. Lab Chip 12, 2469–2486.
Das, J., Ivanov, I., Montermini, L., Rak, J., Sargent, E.H., Kelley, S.O., 2015. Nat. Chem. 7, 569–575.
Dirks, R.M., Pierce, N.A., 2004. Proc. Natl. Acad. Sci. USA 101, 15275–15278.
Dong, H., Jin, S., Ju, H., Hao, K., Xu, L.P., Lu, H., Zhang, X., 2012. Anal. Chem. 84, 8670–8674.
Drummond, T.G., Hill, M.G., Barton, J.K., 2003. Nat. Biotechnol. 21, 1192–1199.
Du, Y., Dong, S., 2017. Anal. Chem. 89, 189–215.
Enkin, N., Wang, F., Sharon, E., Albada, H.B., Willner, I., 2014. ACS Nano 8, 11666–11673.
Ge, S., Zhao, J., Wang, S., Lan, F., Yan, M., Yu, J., 2018. Biosens. Bioelectron. 102, 411–417.
Guo, J., Yuan, C., Yan, Q., Duan, Q., Li, X., Yi, G., 2018. Biosens. Bioelectron. 105, 103–108.
Heid, C.A., Stevens, J., Livak, K.J., Williams, P.M., 1996. Genome Res. 6, 986–994.
Hindson, C.M., Chevillet, J.R., Briggs, H.A., Gallichotte, E.N., Ruf, I.K., Hindson, B.J., Vessella, R.L., Tewari, M., 2013. Nat. Methods 10, 1003–1005.
Ikbal, J., Lim, G.S., Gao, Z., 2015. Trends Anal. Chem. 64, 86–99.
Jung, C., Ellington, A.D., 2014. Acc. Chem. Res. 47, 1825–1835.
Ko, L.J., Prives, C., 1996. Genes Dev. 10, 1054–1072.
Li, B., Ellington, A.D., Chen, X., 2011. Nucleic Acids Res. 39, e110.
Liu, J., Cao, Z., Lu, Y., 2009. Chem. Rev. 109, 1948–1998.
Liu, S., Liu, T., Wang, L., 2015. Chem. Commun. 51, 176–179.
Liu, S., Fang, L., Wang, Y., Wang, L., 2017. Anal. Chem. 89, 3108–3115.
Liu, X., Wang, F., Aizen, R., Yehezkeli, O., Willner, I., 2013. J. Am. Chem. Soc. 135, 11832–11839.
Nie, J., Zhao, M.Z., Xie, W.J., Cai, L.Y., Zhou, Y.L., Zhang, X.X., 2015. Chem. Sci. 6, 1225–1229.
Orbach, R., Guo, W., Wang, F., Lioubashevski, O., Willner, I., 2013. Langmuir 29, 13066–13071.
Qiu, Z., Shu, J., He, Y., Lin, Z., Zhang, K., Lv, S., Tang, D., 2017a. Biosens. Bioelectron. 87,

18–24.
Qiu, Z., Shu, J., Tang, D., 2017b. Anal. Chem. 89, 5152–5160.
Qiu, Z., Shu, J., Tang, D., 2018. Anal. Chem. 90, 1021–1028.
Schena, M., Shalon, D., Davis, R.W., Brown, P.O., 1995. Science 270, 467–470.
Shu, J., Qiu, Z., Lv, S., Zhang, K., Tang, D., 2018. Anal. Chem. 90, 2425–2429.
Smith, S.J., Nemr, C.R., Kelley, S.O., 2017. J. Am. Chem. Soc. 139, 1020–1028.
Wang, F., Elbaz, J., Orbach, R., Magen, N., Willner, I., 2011. J. Am. Chem. Soc. 133, 17149–17151.
Weizmann, Y., Beissenhirtz, M.K., Cheglakov, Z., Nowarski, R., Kotler, M., Willner, I., 2006. Angew. Chem. Int. Ed. 45, 7384–7388.
Xiao, Y., Lai, R.Y., Plaxco, K.W., 2007. Nat. Protoc. 2, 2875–2880.
Yin, B.C., Liu, Y.Q., Ye, B.C., 2013. Anal. Chem. 85, 11487–11493.
Yang, C., Shi, K., Dou, B., Xiang, Y., Chai, Y., Yuan, R., 2015. ACS Appl. Mater. Interfaces 7, 1188–1193.
Yin, P., Choi, H.M.T., Calvert, C.R., Pierce, N.A., 2008. Nature 451, 318–322.
Zhang, D.Y., Seelig, G., 2011. Nat. Chem. 3, 103–113.
Zhang, K., Lv, S., Lin, Z., Li, M., Tang, D., 2018. Biosens. Bioelectron. 101, 159–166.
Zhang, L., Zhu, J., Zhou, Z., Guo, S., Lia, J., Dong, S., Wang, E., 2013. Chem. Sci. 4, 4004–4010.
Zhang, Y., Wang, L., Luo, F., Qiu, B., Guo, L., Weng, Z., Lin, Z., Chen, G., 2017. Chem. Commun. 53, 2910–2913.
Zhang, Y., Zhang, C.Y., 2012. Anal. Chem. 84, 224–231.
Zhao, W.W., Xu, J.J., Chen, H.Y., 2014. Chem. Rev. 114, 7421–7441.
Zhao, Y., Chen, F., Li, Q., Wang, L., Fan, C., 2015. Chem. Rev. 115, 12491–12545.
Zhou, Q., Lin, Y., Zhang, K., Li, M., Tang, D., 2018. Biosens. Bioelectron. 101, 146–152.